Proceedings of the 2nd International Conference on Fluid Flow and Thermal Science (ICFFTS'21)
~~Seoul, South Korea~~ Virtual Conference - November 24- 26, 2021
Paper No. 112
DOI: 10.11159/icffts21.112

Numerical Solution for Inertial Corner Flows in a Fluid Superposed Porous Layer

Abhijit Verma
Indian Institute of Science Bangalore
C. V. Raman Road, Bengaluru-560012, India
abhijitverma@iisc.ac.in

Abstract **–** Solution for the inertial incompressible flow along a right-angle corner in a fluid superposed porous layer is obtained based on single domain formulation. Generalized momentum equation which reduces to Navier-Stokes equation in pure fluid layer is employed to model the inertial flow behaviour in conjugate fluid-porous medium. The governing equations are solved using a second-order projection scheme on quadtree grid. We present flow characteristics for both constant and variable porosity layer for Re = 100. For a given reference Darcy number $Da_0 = 10^{-2}$, it is observed that streamlines crowd near the corner and bottom wall for porous layer with uniform porosity (ε = 0.6) unlike for the case with porosity varying linearly across the layer (ε = 0.2-1.0). Furthermore, the velocity field is seen exhibiting similarity behaviour for both constant and variable porosity layers. In the absence of any exact solutions for non-linear inertial porous flows, the existence of similarity solution in case of corner flows in a fluid overlying porous layer serves as a reliable theoretical tool to verify the numerical scheme for solving the conservation equations describing inertial flows through heterogeneous porous media.

Keywords**:** Inertial flows, Corner geometry, Variable porosity, Fluid superposed porous layer

1. Introduction

Corner flows in a fluid superposed porous medium find several applications in industrial and natural processes such as porous bearings, heat exchangers, alloy solidification, nuclear reactors etc. In these applications, fluid flow ranges from creeping to inertial regime and the properties of the porous medium might vary spatially. In creeping flow regime, Bars and Worster [1] reported similarity solution of Darcy-Brinkmann equation analytically and numerically for corner flow in a fluid overlying porous layer with constant and variable porosity respectively. However, to our knowledge, no solutions are available in the literature to corner flow problems with inertial effects in fluid overlying porous media.

In this paper, we present numerical solution for the inertial corner flow in a fluid superposed porous layer, both with a constant porosity and with a linear porosity variation in transverse direction. The solutions for both the cases are compared to assess the effect of porosity variation on flow field in the corner geometry. Also, the velocity profiles across the fluid-porous layer are analysed for different longitudinal positions. Here, based on single domain formulation, fluid flow in the composite system is modelled by generalized momentum equation. The partial differential equations are solved with second order accuracy.

2. Equations and Method of Solution

As shown in Figure 1, we compute velocity field $\mathbf{u}(x, y)$ in a two-dimensional rectangular domain (0, 10) × (0, 1) with porous medium present in (0, 10) × (0, 0.5). Adopting single-domain approach, flow in the entire domain is captured by generalized porous flow model. Therefore, the non-dimensional continuity and momentum equations are given as [2, 3]

$$\nabla \cdot \mathbf{u} = 0 \tag{1}$$

$$\frac{\partial \mathbf{u}}{\partial t} + \mathbf{u} \cdot \nabla \left(\frac{\mathbf{u}}{\varepsilon}\right) = -\varepsilon \nabla \mathrm{p} + \varepsilon \nabla \cdot \frac{2}{\varepsilon \mathrm{Re}} \mathbf{S} - \frac{(1-\varepsilon)^2}{\varepsilon^2 \mathrm{Da}_0 \mathrm{Re}} \mathbf{u} - \frac{0.143(1-\varepsilon)}{\varepsilon^2 \sqrt{\mathrm{Da}_0}} |\mathbf{u}|\mathbf{u} \tag{2}$$

where ε, Da_0, Re, and $\mathbf{S}$ are porosity, reference Darcy number, Reynold number, and non-dimensionalized deformation tensor. In (2), the last two terms are referred to as viscous and inertial drags caused by the porous medium. The dimensionless parameter Da_0 is defined as $\mathrm{Da}_0 = \frac{\mathrm{D}^2}{150}$; where D is dimensionless pore diameter.

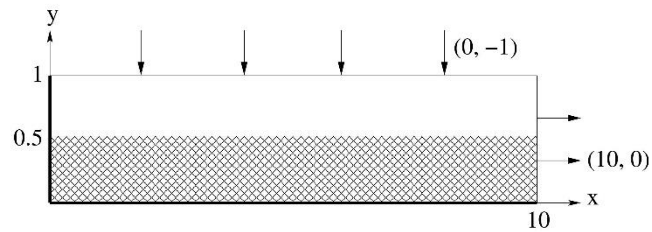

Fig. 1: Computational domain for corner flow in a fluid superposed porous medium.

The boundary conditions are written as

$$\begin{aligned} &u = 0, && v = -1 && \text{at } y = 1; \\ &u = 10, && v = 0 && \text{at } x = 10; \\ &u = 0, && \nabla_x v = 0 && \text{at } x = 0; \\ &\nabla_y u = 0, && v = 0 && \text{at } y = 0; \end{aligned} \quad (3)$$

We solve the set of equations (1) - (2) with boundary conditions (3) using projection algorithm proposed by Bell et al. [4] on cell-centred quadtree grid in finite volume framework. To obtain face-centred velocity field, the scheme employs Godunov type procedure which doesn't pose any cell Reynold number stability criterion, thereby providing a robust discretization for inertial flows. Making use of limiter in slope computations prevents the scheme from producing spurious oscillations in presence of discontinuity in porosity field. Moreover, balanced-force scheme is applied to ensure exact (discrete) equilibrium between pressure gradient and viscous as well as inertial drags. The system of algebraic equations is solved by multi-grid accelerated Gauss-Seidel method. Taking zero velocity field as the initial condition, we march in time until the solution reaches steady state defined as $||u_j^{n+1} - u_j^n||_{L_1} < 10^{-7}$; where *n* is the time level, *j* is the cell index, and $||.||_{L_1}$ denotes first norm in *L*-space. For the quantitative validation of the numerical scheme for fluid superposed porous media, we compare our result for Couette flow without non-linear inertial drag against the analytical solution of Martys et al. [5] in Figure 2. The comparison shows excellent agreement between the numerical and analytical solutions.

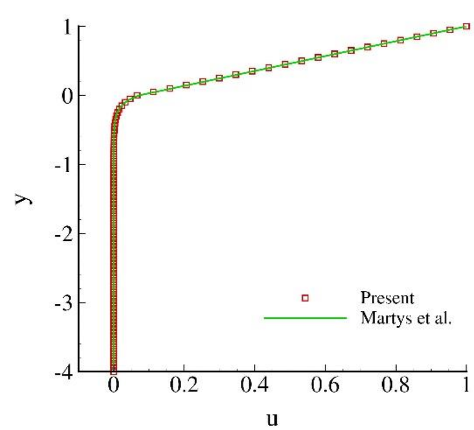

Fig. 2: Comparison of *u*-velocity profile against analytical solution of Martys et al. [5] for Couette flow with $\varepsilon = 0.5$ and $\mathrm{Da}_0 = 10^{-2}$.

3. Results and Discussion

In this section, we present simulation results for porous layer with porosity $\varepsilon = 0.6$ and $\varepsilon = 0.2 + 1.6y$ for Re = 100 and $\mathrm{Da}_0 = 10^{-2}$. Computational domain, shown in Figure 1, is discretized using grid size $2^{-6}/2^{-8}$ with finer resolution near the interface.

The time step is taken as 10^{-5}. The streamline patterns obtained for both constant and variable porosity cases are shown in Figure 3. As it is seen, streamlines crowd near the corner and bottom boundary in case of constant porosity layer while they drift away for variable porosity layer. This happens because the resistance to flow vary significantly across the layer in case

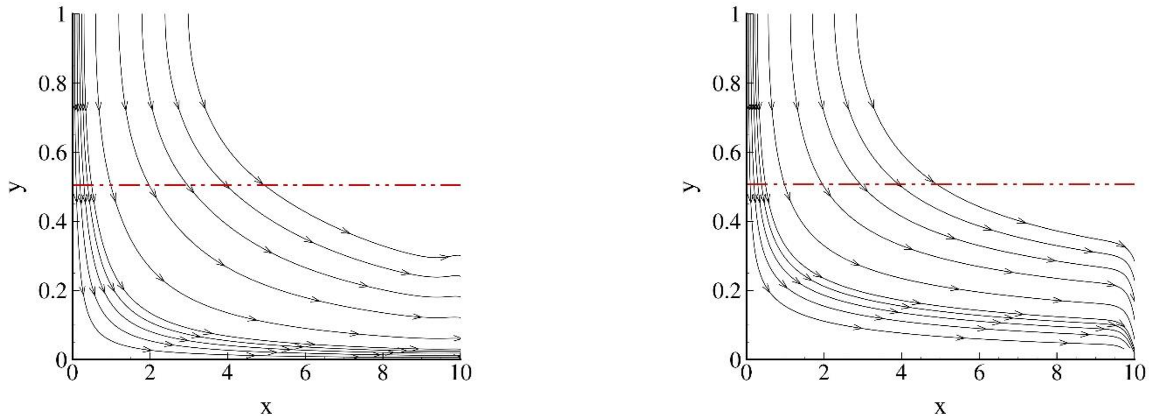

Fig. 3: Streamline pattern in a section of computational domain for: Left) constant porosity layer; and Right) variable porosity layer. The line in red represents the interface between fluid and porous layers.

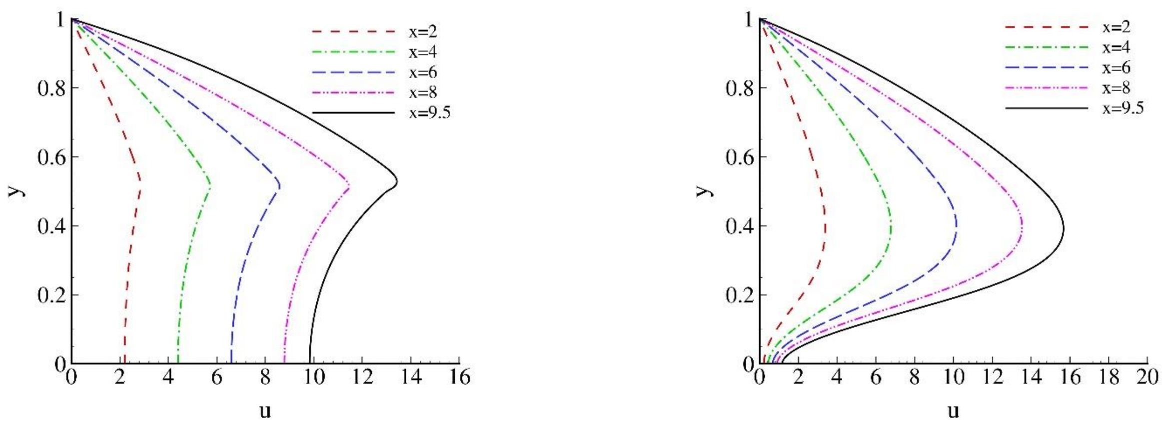

Fig. 4: *u*-velocity profiles with x for: Left) constant porosity layer; and Right) variable porosity layer.

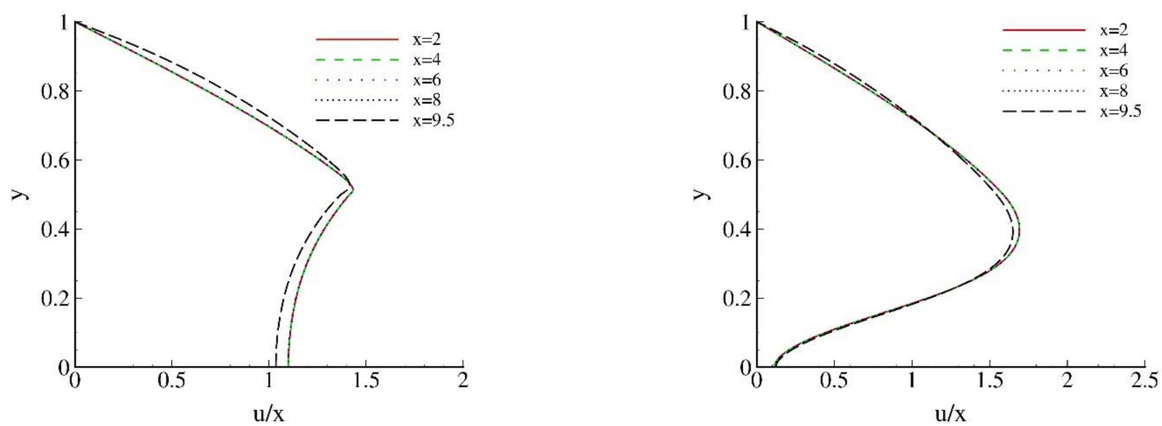

Fig. 5: Scaled *u*-velocity profiles with x for: Left) constant porosity layer; and Right) variable porosity layer.

of variable characteristics and fluid with high inertia chooses path that offers lesser drags. Because of this behaviour, evident from the change in gap between two successive streamlines, volume flow rate across the inhomogeneous porous layer also vary considerably. This is further illustrated by the *u*- and *v*-velocity profiles shown in Figures 4 - 6.

In Figure 4, change in *u*-velocity profiles with longitudinal positions are shown. It is evident that *u*-velocity and consequently volume flow rate across any transverse section increases with distance from the corner for both constant and variable porosity layers. This behaviour is desirable to ensure mass conservation. In Figure 5, scaled *u*-velocity profiles at different longitudinal positions collapse into a single curve except the one near the exit boundary. *v*-velocity profiles show the same trend as shown in Figure 6. Collapsing of all *u*- and *v*-velocity profiles (but the ones near the outlet) to the same curve suggests the existence of similarity solution in the form $\mathbf{u} = [x\, f(y), g(y)]$.

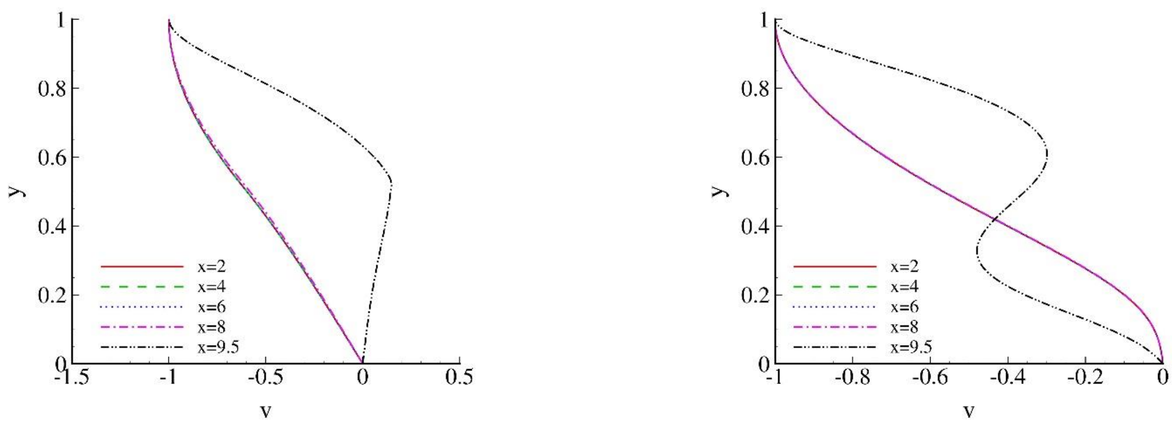

Fig. 6: *v*-velocity profiles with x for: Left) constant porosity layer; and Right) variable porosity layer.

4. Conclusion

We have presented solution for incompressible flow with inertial effects along a right-angle corner in a fluid overlying porous layer with constant and variable porosity. For a given reference Darcy number, the density of streamlines near the corner and bottom boundary is much higher in case of uniform porosity layer as compared to variable porosity scenario with mean value equal to porosity for homogeneous layer. Moreover, both *u*- and *v*-velocity fields show similar profile in longitudinal direction which can serve as a theoretical tool for the qualitative verification of solution methodology. Therefore, we believe that the similarity solutions presented in this paper could be used to validate the computer code simulating inertial flow in heterogeneous porous medium.

References

[1] Michael Le Bars and M Grae Worster. Interfacial conditions between a pure fluid and a porous medium: implications for binary alloy solidification. *Journal of Fluid Mechanics*, 550:149–173, 2006.

[2] Zhaoli Guo and TS Zhao. Lattice boltzmann model for incompressible flows through porous media. *Physical review E*, 66(3):036304, 2002.

[3] Antony A Hill and Magda Carr. Nonlinear stability of the one-domain approach to modelling convection in superposed fluid and porous layers. *Proceedings of the Royal Society A: Mathematical, Physical and Engineering Sciences*, 466(2121):2695–2705, 2010.

[4] John B Bell, Phillip Colella, and Harland M Glaz. A second-order projection method for the incompressible Navier-Stokes equations. *Journal of Computational Physics*, 85(2):257–283, 1989.

[5] N Martys, Dale P Bentz, and Edward J Garboczi. Computer simulation study of the effective viscosity in Brinkmann's equation. *Physics of Fluids*, 6(4):1434–1439, 1994.